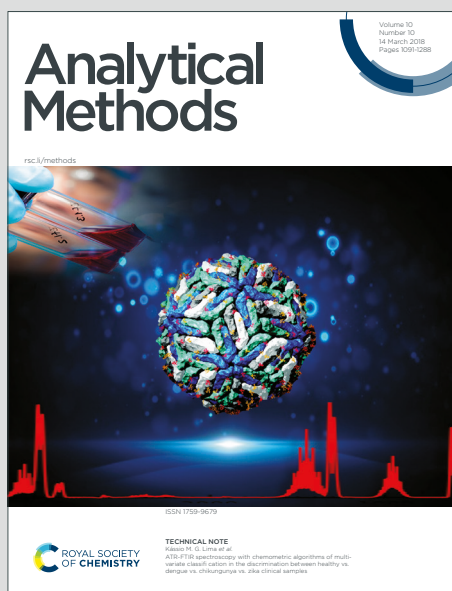


# Analytical Methods

Accepted Manuscript

This article can be cited before page numbers have been issued, to do this please use: L. Gonzalez-Legarreta, C. Renero-Lecuna, R. Valiente and M. L. Fanarraga, *Anal. Methods*, 2020, DOI: 10.1039/D0AY01357A.



This is an Accepted Manuscript, which has been through the Royal Society of Chemistry peer review process and has been accepted for publication.

Accepted Manuscripts are published online shortly after acceptance, before technical editing, formatting and proof reading. Using this free service, authors can make their results available to the community, in citable form, before we publish the edited article. We will replace this Accepted Manuscript with the edited and formatted Advance Article as soon as it is available.

You can find more information about Accepted Manuscripts in the [Information for Authors](#).

Please note that technical editing may introduce minor changes to the text and/or graphics, which may alter content. The journal's standard [Terms & Conditions](#) and the [Ethical guidelines](#) still apply. In no event shall the Royal Society of Chemistry be held responsible for any errors or omissions in this Accepted Manuscript or any consequences arising from the use of any information it contains.

## ARTICLE

## Development of an accurate method for dispersion and quantification of carbon nanotubes in biological media

Lorena González-Legarreta,<sup>a,b</sup> Carlos Renero-Lecuna<sup>a,\*,†</sup>, Rafael Valiente<sup>a,c</sup> and Mónica L. Fanarraga<sup>a,d</sup>Received 00th January 20xx,  
Accepted 00th January 20xx

DOI: 10.1039/x0xx00000x

Understanding the biological effects triggered by nanomaterials is crucial, not only in nanomedicine but also in toxicology. The dose-response relation is relevant in biological tests due to its use for determining appropriate dosages for drugs and toxicity limits. Carbon nanotubes can trigger numerous unusual biological effects, many of which could have unique applications in biotechnology and medicine. However, their resuspension in saline solutions and the accurate determination of their concentration after dispersion in biological media are major handicaps to identify the magnitude of the response of organisms as a function of this exposure. This difficulty has led to inconsistent results and misinterpretations of their *in vivo* behavior, limiting their potential use in nanomedicine. The lack of a proper protocol that allows comparing different studies of the carbon nanotubes content and its adequate resuspension in culture cell media gives rise to this study. Here, we describe a methodology to functionalize, resuspend and determine the carbon nanotubes concentration in biocompatible media based on UV-Vis spectroscopy. This method allows us to accurately estimate the concentration of these resuspended carbon nanotubes, after removing bundles and micrometric aggregates, which can be used as a calibration standard, for dosage-dependent studies in biological systems. This method can also be extended to any other nanomaterial to properly quantify the actual concentration.

### 1 Introduction

Since their first scientific report by S. Iijima in the '90s<sup>1</sup>, carbon nanotubes (CNTs) have been extensively used in many different fields from basic research up to industrial applications. These concentrically bent graphene layers exhibit unique physical and chemical properties, such as high electric and thermal conductivity, strength, stiffness, and toughness<sup>2,3</sup>. One of its most relevant characteristics from the biological point of view is its high Aspect Ratio (AR), length to diameter ratio; where its inner diameter can be as small as 2 nm and the length can range up to several micrometers (AR >> 1000)<sup>3</sup>. This characteristic together with its reactive surface made them useful as nanocarriers. The interior can be used to incorporate molecules or small clusters<sup>4,5</sup>, while its surface can be

decorated with drugs and proteins, making them potential candidates for use as nanocarriers<sup>6-12</sup>.

Furthermore, this high AR<sup>2,3,13</sup> is quite important in nanobiotechnology since these nanofilaments can adsorb a huge mass of proteins on their surfaces<sup>14-16</sup> acquiring different biological identities that entitle their participation in complex biochemical and cellular processes<sup>17,18</sup>. Moreover, well-resuspended individual CNTs can penetrate in tissues and cells, where they biomimetically interact with the intracellular filaments (nucleic acids, actin filaments or microtubules) interfering with their function, triggering antiproliferative<sup>19,20</sup>, antimigratory<sup>20,21</sup> and cytotoxic or proapoptotic effects<sup>22-28</sup> that can be used in the development of smart active-by-design nanocarrier systems in cancer treatment. These nanomaterials assemble mixed bio-synthetic filaments with the biological polymers changing their properties. Remarkably, the diameter of the CNT determines their affinity for one or the other polymer, resulting in different cellular effects. Single-walled CNT (SWCNT) preferably interact with DNA (2 nm wide) or actin (4-7 nm wide), while multi-walled CNTs (MWCNT) are more prompt to interact with microtubules (25 nm diameter). These interactions lead to DNA breaks<sup>25,29-32</sup>, blockade of the cellular biomechanics<sup>20,21,28</sup>, chromosome malsegregation<sup>17,33</sup> as a result of their interference with the DNA<sup>16,30,34,35</sup>, and actin<sup>36-38</sup> or microtubule<sup>17-20</sup> malfunction. Interestingly, all these unique biomimetic properties disappear when CNTs appear into micrometric bundles. Aggregated CNTs behave as micrometric particles, are also endocytosed but trigger

<sup>a</sup> Grupo de Nanomedicina-IDIVAL, Facultad de Medicina, Universidad de Cantabria, Avd. Cardenal Herrera Oria s/n, 39011 Santander, Spain.

<sup>b</sup> Dept. QUIPRE, Inorganic Chemistry-University of Cantabria, Avd. de Los Castros 46, 39005 Santander, Spain.

<sup>c</sup> Dpto. Física Aplicada, Facultad de Ciencias, Universidad de Cantabria, Avd. de los Castros 48, 39005, Santander, Spain.

<sup>d</sup> Dpto. Biología Molecular, Facultad de Medicina, Universidad de Cantabria, Avd. Cardenal Herrera Oria s/n, 39005, Santander, Spain

\* Corresponding author. E-mail: crenero@idival.org (Carlos Renero-Lecuna)

† Present address: CIC biomaGUNE, Paseo Miramón 182, Donostia - San Sebastián 20009, Spain.

Electronic Supplementary Information (ESI) available: [details of any supplementary information available should be included here]. See DOI: 10.1039/x0xx00000x

cytotoxicity by different means<sup>39,40</sup> often as a result of an overdose of nanomaterial per cell.

Knowing the exact dose of nanotubes applied in a study is critical to understand their effect. Many studies referring to the concentration-dependent cytotoxic effects of CNTs use dosages much higher than what might be physiologically relevant (as the basic principle of toxicity states: “the dose makes the poison”). In many cases, concentrations above 200 or 400  $\mu\text{g}/\text{ml}$  are reported<sup>41</sup>. However, at these concentrations, it is difficult to conciliate/assume that CNTs are not aggregated in micrometric bundles rather than well dispersed. Existing literature demonstrates how these nanotubes are aggregated, packed into bundles, or bind to other nano/micrometric structures, changing their interaction with cells and their intracellular components (e.g. microtubules)<sup>42</sup> in comparison with the effects when the CNTs are completely dispersed and elongated<sup>43</sup>.

Traditionally, CNTs have been weighed and resuspended from dry powder. The CNTs resuspension has been generally performed using an ultrasonication probe in the dispersant media<sup>44</sup>. Unfortunately, the amount of salt present in physiological media (containing typically 150 mM NaCl) and the heterogeneity of the CNTs preparations, often lead to partial aggregation of the sample, which should be eliminated by low-speed centrifugation, thus resulting in a fractional loss of the initial CNTs suspension. This leads to inaccurate conclusions between experiments performed in different laboratories, or even in the replicas of the same laboratory.

In this paper, we describe an effective and reproducible protocol to optimally functionalize CNTs, eliminate the aggregates from the suspension using moderate centrifugation steps and, finally, a reproducible laboratory technique, based on ultraviolet-visible (UV-Vis) spectroscopy, for accurate quantification of the dispersed CNTs in suspension ready to use for the biological assays.

Although we have optimized the method for CNTs (different types including single-walled, pristine- or oxidized-multiwalled carbon nanotubes) it can be used to estimate the concentration of different carbon allotropes, such as graphene oxide suspensions. Nonetheless, it is also opened to determine the concentration of any other kind of nanomaterial displaying strong light scattering in the visible spectral region (400 – 800 nm). This range has been established because most low-cost and commercially available spectrometers often used in labs can work at these wavelengths.

## 2 Experimental

### 2.1 Materials

**High-purity (95%+) multiwalled-carbon nanotubes (MWCNTs) dry powders were purchased from Nanocyl, pristine (p-MWCNT, ref. NC3100) and oxidized MWCNT (o-MWCNT, ref. NC3101). High-purity single walled-carbon nanotubes (SWCNTs) dry powders were purchased from Sigma Aldrich**

**(ref. 900711) and used as prepared. Colourless culture cell media DMEM (Dulbecco Modified Eagle's Medium) without phenol red, with glucose, sodium pyruvate and carbonic buffer  $\text{NaHCO}_3$  from PAN biotech® and Fetal Bovine Serum (FBS) from TICO Europe® were used as dispersant biological media for the CNT dry powders, (DMEM-FBS).**

### 2.2 Characterization methods

High-purity CNTs samples were morphologically characterized using Transmission Electron Microscopy (TEM) and Raman spectroscopy. TEM measurements were carried out with a JEOL JEM 1011 operating at the maximum voltage of 80 kV. The suspended and functionalized nanotubes were washed in bi-distilled water by centrifugation at 20,000 g for 1 hour, 3 times, then resuspended and deposited onto 400 mesh carbon-coated copper grids. Raman measurements were performed with a JASCO NRS-4500 Confocal Raman Microscope under 532 nm excitation wavelength. The light is collected with a 100x objective and dispersed with a 900 grooves/mm grating and detected with an Andor Newton CCD detector refrigerated with Peltier at  $-70^\circ\text{C}$ . The laser power on the sample is less than 10 mW to avoid sample damage by laser heating. UV-Vis absorption spectra to obtain the calibration curves were collected by a double-beam Cary6000i spectrophotometer and a single beam Cary50. All samples were measured using semi-micro PS cuvettes of 1.5 ml and 10 mm of path length of Deltalab. A bench-top Biochrom Libra S2 model colorimeter was also used to measure the absorbance of the CNTs supernatant suspensions to determine the content of CNTs in the dispersion before to administrate to cell cultures.

### 2.3 Functionalization protocol for calibration curve measurements

To prepare the fine dispersion of the CNTs to measure the calibration curve, first, the CNTs dry powders (p-MWCNT, o-MWCNT and SWCNTs) are weighed on a precision scale. Small amounts of CNTs (typically around 1 mg) are used to avoid large volumes of dispersant media ensuring that all CNTs are well dispersed. Then the CNTs dry powder is transferred to a 15 ml centrifuge conical tube and an amount of 10 ml of DMEM (without phenol red) media containing 30% FBS (DMEM-FBS) is added with a precision pipette. In our case, the mixture was exposed to at least 4 cycles of 4 minutes of mild sonication (Sonics Vibra-cell model 75185) at 91 W. Sonication steps must be carried out on an ice bath (ca.  $4^\circ\text{C}$ ) to prevent the serum protein denaturation and coagulation. To remove microaggregates of CNTs, the suspension is low-speed centrifuged at 12,000 g for 10 minutes at  $4^\circ\text{C}$ . After centrifugation, the supernatant containing the well-suspended CNTs can be stored at  $4^\circ\text{C}$  until use. Depending on the CNT type as well as other variables (serum concentration, temperature, sonication probe/intensity, etc.), the sonication – centrifugation step can be repeated several times (as much

as required) until there is no pellet in the centrifuge tube after the 12,000g – 10 minutes centrifugation (Figure 1). In every step, the CNTs pellet is resuspended with at least 10 ml of fresh media, though the same media could be used for resuspension if a higher concentration of CNTs is required. For the standard calibration curve measurement purposes, we have used a total volume ca. 60 ml of dispersant media to perfectly disperse ca. 1 mg of CNTs dry powder (although it can vary depending on the type of CNT used). After resuspension, the stability of the CNTs dispersions is tested by UV-Vis absorption spectra in the 300–800 nm range. The resulting CNTs dispersions can be stored at 4°C for several months without any further treatment (see Video S4 that shows the easy resuspension of the SWCNT in distilled water, for example).

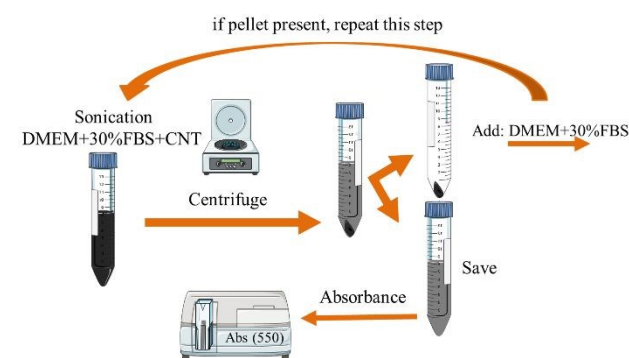


**Figure 1:** Protocol of CNTs dispersion in DMEM – FBS for curve calibration preparation. The upper arrow represents an iterative procedure that can be repeated until there is no pellet formed in the tube.

## 2.4 Calibration curve measurements

Upon complete dispersion, a final volume of 800  $\mu$ l CNT suspension of known concentration was loaded in the absorption cuvettes and different aliquots with different dilution ratios are prepared to be measured in the absorption cuvettes. The dilution media is the same as the resuspended media (DMEM-FBS). Previously to the absorption measurements, the CNTs suspensions are bath-sonicated to assure the homogeneity. The UV-Vis absorption spectra of the different samples were collected in the 300–800 nm spectral range, using the DMEM-FBS diluting media as a reference with the same (single beam spectrophotometer) or a twin cuvette with the CNTs suspension (double-beam one). In our case, the wavelength selected to build our calibration curves is 550 nm. Interestingly, this wavelength should be selected in such a way that the dispersion media does not absorb at these wavelengths. Our media DMEM-FBS absorbs between 380 – 440 nm (see Figure S1).

## 2.5 Functionalization of CNTs for biological experiments

To prepare from scratch the dispersion of functionalized CNTs of a known concentration for experimental purposes, i.e., for cell culture administration; first, a stock suspension of the dispersant media (DMEM-FBS) with a high concentration of CNTs is prepared. For this purpose, an appropriate amount of CNTs are dispersed in fresh media. Then, a moderate 3 minutes mild sonication at 130 W on an ice bath to prevent protein from coagulation is performed. Afterward, the suspension is low-speed centrifuged at ca 12,000 g for 10 minutes and the supernatant, which contains the functionalized nanotubes, is collected for analysis. The absorbance of this supernatant is measured with a bench-top spectrometer at a fixed wavelength (typically at 550 nm) using the dispersant media, DMEM-FBS as reference. Using the obtained calibration curve (section 2.4 of Experimental), the concentration of the resuspended CNTs can be determined. Often, the initial suspension of nanotubes is too concentrated, when this happens, a diluted sample of the as-prepared dispersed CNTs dispersion is measured (i.e., it can be diluted 1:10, 1:50 or more). In summary, the sonication step followed by the low-speed centrifugation procedures ensure a sufficient CNTs functionalization and its perfect dispersion in saline media, preventing the aggregation or the presence of micrometric CNT bundles (aggregates), while preserving the unidimensional morphology of these materials.

## 3 Results and Discussion

The quality of the commercially as-prepared CNTs used in our experiments was examined by TEM and Raman spectroscopy. Figure S2 shows images of p-MWCNTs, o-MWCNTs and SWCNT from Nanocyl and Sigma, respectively (see Experimental). These figures allow the estimation of the outer diameter of the CNTs, ca. 6 nm. Raman spectra of p-MWCNTs, o-MWCNTs and SWCNT are shown in Figure 2 (left). These typically consist of two intense bands and an overlapping weaker shoulder in the 1000  $\text{cm}^{-1}$  to 1800  $\text{cm}^{-1}$  range. The two most intense peaks are assigned to the D and G bands at around 1340 and 1580  $\text{cm}^{-1}$ . They are related to the defects in the structure (D) and the in-plane bond-stretching modes that come from the graphene sheet that bends to form the carbon nanotube (G). Also, a replica of the defect D band is measured (D') at around 1608  $\text{cm}^{-1}$ .

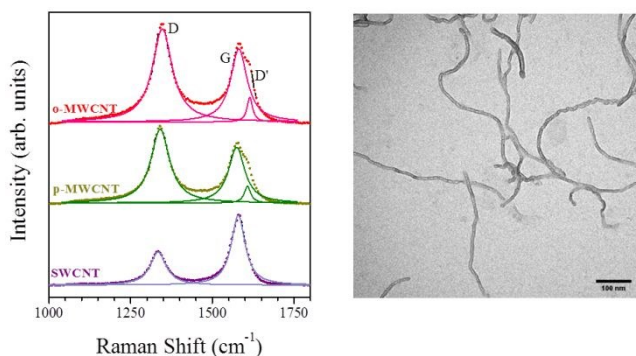


**Figure 2.-** Convolution of the Raman spectra of the p- and o-MWCNT in Lorentzian function (see text) probing the oxidation state of the sample and SWCNTs (left) and TEM images of the functionalized and dispersed o-MWCNTs after centrifugation step proposed in our protocol (right).

The ratio between the D and G bands depends on the oxidation state and surface defects of the nanotubes<sup>45</sup>. This ratio is an indication of the defects concentration on the CNTs surface and increases with the oxidation degree of the CNTs. Accordingly, the D' intensity band increase in the o-MWCNT compared to the p-MWCNT. For the SWCNT, band D' is not appreciable even after band convolution and the intensity of the G band is approximately twice more intense than band D associated with defects. Figure 2 (right) shows a representative TEM image of the functionalized and well-dispersed o-MWCNTs, after the centrifugation step, no micro-aggregates are present. Before the low-speed centrifugation step (Figure S3), some MWCNTs aggregations are observed (black-spots-like) together with the well-dispersed nanotubes and some darker dots due to the crystallization of the salts present in the culture cell media. In contrast, in the low-speed centrifuged o-MWCNTs (Figure 2 right), the aggregates have disappeared and only the well-dispersed o-MWCNTs are observed.

Depending on the CNTs type (oxidized, pristine, single-walled, multi-walled, etc.), resuspension can be tough. Sonication in the presence of serum proteins helps resuspension by functionalizing the nanotube surfaces and it is an easy and efficient way to disperse MWCNTs and SWCNTs to use them in biological experiments, i.e. tissue culture tests. Upon dispersion and functionalization of the CNTs as explained in the experimental method (described in section 2.3 of Experimental), it is observed an almost opaque black liquid that can be cleared upon successive dilutions (Figure 3). This change in the appearance of the suspension can be used to determine the concentration of CNTs present in the suspension, through the measurement of the absorbance.

p-MWCNTs, o-MWCNTs and SWCNTs dispersions show the absorption spectra with the characteristic scattering behaviour (Figure S1), where no absorption bands are expected. This scattering is directly related to the concentration of CNTs. Therefore, it is possible to estimate the concentration of CNTs

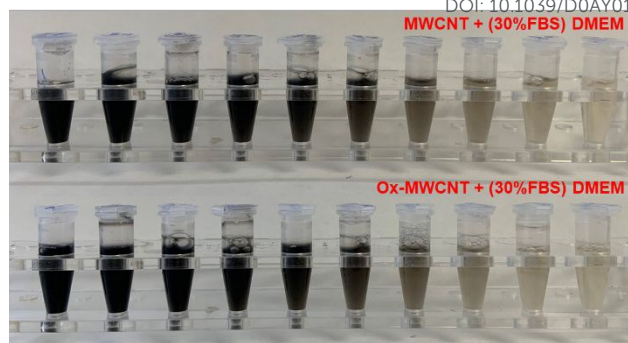


**Figure 3.-** p-MWCNTs and o-MWCNT perfectly dispersed in DMEM-FBS. The different colours of the suspensions are indicative of the different concentrations of CNTs in suspension.

in the suspension using the standard calibration curve, just acquiring the UV-Vis absorption spectra. The characteristic increase of absorption at lower wavelengths is related to the Rayleigh scattering, which shows a wavelength dependence as  $\lambda^{-4}$ , and depends on the sample shape and size (Figure S1)<sup>46</sup> and sometimes is referred to as turbidity.

To represent the calibration curve, the absorption spectra of the samples prepared with different known concentrations of CNTs are collected (Figure 4) and representing the absorbance value at a particular wavelength. Here we have selected the absorbance at 550 nm since it is the standard configuration for most bench-top colorimetry equipment, but any other wavelength can be selected since the whole absorbance spectra (350-800 nm range) were measured.

Figure 4 displays the Lambert-Beer calibration plot for p-MWCNTs and o-MWCNTs as well as SWCNTs obtained through the absorption value at 550 nm.

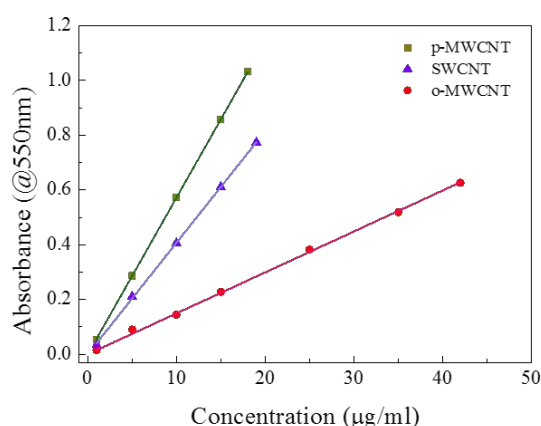


**Figure 4.-** Absorbance standard curve established from a suspension of pristine, oxidized MWCNTs and SWCNT dispersed in DMEM-FBS.

The calibration curves of p-MWCNTs, o-MWCNTs and SWCNTs (values in Table 1), showed in Figure 4, allow a good estimation of the CNTs concentration after centrifugation. It is worth noting that the different CNTs present different slopes in the curves, which is correlated with its capability of being dispersed in the media. The o-MWCNTs, with the lowest slope ( $a = (1.497 \pm 0.013) \times 10^{-2} \mu\text{g/ml}$ , Table 1), present the highest capability of dispersion in the media meanwhile the pristine ones are harder to dispersed and therefore its  $a$  coefficient is the highest (Table 1).

**Table 1.-** Curve fitting coefficients of the three CNTs suspensions measured at 550 nm at RT in a DMEM-30% FBS solution, obtained from Fig. 3. All the fittings have an  $R^2 > 0.998$ .

	$a \times 10^2 (\mu\text{g/ml})$	$\Delta a \times 10^2 (\mu\text{g/ml})$
p-MWCNT	5.720	0.012
SWCNT	4.078	0.019
o-MWCNT	1.497	0.013

This difference in the dispersibility of the CNTs in the same media, as inferred by their different  $a$  coefficient, is due to their previous chemical surface functionalization. In the case of the o-MWCNTs, due to the oxidation process of its surface, display more active groups in their large surface, mainly hydroxyl-groups, what means that they have more bonding sites, being able to capture some ions and the proteins from the media and, therefore, being more easily dispersible<sup>47,48</sup>. Interestingly, there is a saturation concentration for each system at which the plots (Figure 4) will lose its linear behaviour, indicating the maximum amount of CNTs that is possible to resuspend without forming aggregates. For this reason, it should be always checked the linearity of the absorbance before taking the concentration value. We can do it by just diluting our sample and checking that the absorbance decrease linearly i.e. sample diluted 10%  $\rightarrow$  absorbance decreases 10%.

This easy method to measure the concentration of a suspension/dispersion of CNTs, using the absorbance spectra, can also be applied in other systems, measuring the turbidity, where the scattering of light is due to the small particles present in the media, and comparing the absorption value with previously standard curves prepared *ad hoc*. In this way, the described method could be applied for determining the concentration of liposomes, graphene oxide, carbon dots, etc.

## Conclusions

Here we develop an effective and quick method for biological functionalization and accurate determination of the concentration of CNTs in culture media containing serum proteins. This functionalization technique disperses CNTs individually and helps in their resuspension and stabilization in saline solutions, endowing CNTs with a biological identity that is key in many biological applications. Using the absorption

measurements, it is feasible to determine the exact concentration of CNTs in these suspensions, and thus the exact concentration of CNTs administrated to the cell culture. The advantage of this method overall is that it is not only valid for CNTs and could also be easily extended to other nanomaterials that present light scattering within the region of interest.

## Conflicts of interest

There are no conflicts to declare.

## Acknowledgements

This work has been funded by the Instituto de Salud Carlos III (ISCiii) (ref. PI16/00496, PI19/00349, DTS19/00033); co-funded by ERDF/ESF, "Investing in your future"; the Spanish MINECO (project ref. PGC2018-101464-B-I00) and MICINN NanoBioApp Network (MINECO-17-MAT2016-81955-REDT). Authors also thank the networks Raman4Clinics (BM1401). CRL thanks the MINECO for the Juan de la Cierva Formación grant (ref. FJCI-2015-25306) and LGL the ISCiii for the Sara Borrell grant (ref. CD17/00105). The authors want to also thank the IDIVAL for financial support (refs. NVAL18/07, INNVAL18/28) and technical support.

## Notes and references

- S. Iijima, *Nature* 1991, **354**, 56–58.
- T. W. Ebbesen, H. J. Lezec, H. Hiura, J. W. Bennett, H. F. Ghaemi, T. Thio, *Nature* 1996, **382**, 54–56.
- V. N. Popov, *Mat. Sci. and Eng. R: Reports* 2004, **43**, 61–102.
- E. del Corro, M. Taravillo, J. González, V.G. Baonza, *Carbon* 2011, **49**, 973–979.
- E. Belandria, M. Millot, J.M. Broto, E. Flahaut, F. Rodriguez, R. Valiente, J. González, *Carbon* 2010, **48**, 2556.
- E. González-Lavado, L. Valdivia, A. García-Castaño, F. González, C. Pesquera, R. Valiente, M.L. Fanarraga, *Oncotarget* 2019, **10**, 2022–2029.
- T. Kopac, K. Bozgeyik, E. Flahaut, *J. Mol. Liquids* 2018, **252**, 1–8.
- N. W. S Kam, T. C. Jessop, P. A. Wender, H. Dai, *J. Am. Chem. Soc.* 2004, **126**, 6850–1.
- X. Luo, C. Matranga, S. Tan, N. Alba, X. T. Cui, *Biomaterials* 2011, **32**, 6316–23.
- Z. Zhang, X. Yang, Y. Zhang, B. Zeng, S. Wang, T. Zhu, Richard B.S. Roden, Yongsheng Chen, Rongcun Yang, *Clin Cancer Res.* 2006, **12**, 4933–4939.
- G. Bardi, A. Nunes, L. Gherardini, K. Bates, K. T. Al-Jamal, C. Gaillard, M. Prato, A. Bianco, T. Pizzorusso, K. Kostarelos, *PLoS One.* 2013, **8**, e80964.
- C. Klumpp, K. Kostarelos, M. Prato, A. Bianco, *Biochimica et Biophysica Acta (BBA) - Biomembranes*, 2006, **1758**, 404–412.
- A. Peigney, C. Laurent, E. Flahaut, R.R. Bacsá, A. Rousset, *Carbon* 2001, **39**, 507–514.
- X. Cai, R. Ramalingam, H. S. Wong, J. Cheng, P. Ajuh, S.H. Cheng, Y. W. Lam, *Nanomed-Nanotechnol* 2013, **9**, 583–593.
- J. H. Shannahan, J. M. Brown, R. Chen, P. C. Ke, X. Lai, S. Mitra, F. A. Witzmann, *Small* 2013, **9**, 2171–2181.
- Z. Yang, L. Deng, Y. Lan, X. Zhang, Z. Gao, C.W. Chu, Dong Cai, and Zhifeng Ren, *PNAS* 2014, **111**, 10966–10971.
- L. Rodríguez-Fernández, R. Valiente, J. González, J. C. Villegas, M. L. Fanarraga, *ACS Nano* 2012, **6**, 6614–6625.

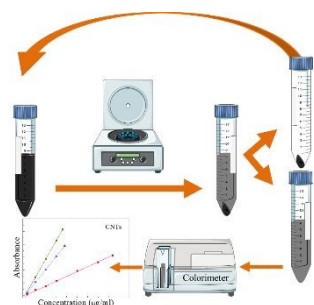
- 18 F. Pampaloni, E. L. Florin, *Trends Biotechnol.* 2008, **6**, 302–210.
- 19 L. García-Hevia, F. Fernández, C. Grávalos, A. García, J. C. Villegas, M. L. Fanarraga, *Nanomedicine* 2014, **9**, 1581–1588.
- 20 C. Dong, R. Eldawud, L. M. Sargent, M. L. Kashon, D. Lowry, Y. Rojanasakul, C. Z. Dinu, *J. Mater. Chem. B* 2015, **3**, 3983–3992.
- 21 L. García-Hevia, R. Valiente, J. L. Fernández-Luna, E. Flahaut, L. Rodríguez-Fernández, J. C. Villegas, J. González, M. L. Fanarraga, *Adv. Healthc. Mater.* 2015, **4**, 1640–1644.
- 22 R. K. Srivastava, A. B. Pant, M. P. Kashyap, V. Kumar, M. Lohani, L. Jonas, Q. Rahman, *J. of Nanotox* 2011, **5**, 195–207.
- 23 A. R. N Reddy, Y. N. Reddy, D. R. Krishna, V. Himabindu, *Toxicology*. 2010, **272**, 11–16.
- 24 H. Ali-Boucetta, K. T. Al-Jamal, K. Kostarelos, *Methods Mol Biol.* 2011, **726**, 299–312.
- 25 Y. Y. Guo, J. Zhang, Y. F. Zheng, J. Yang, X. Q. Zhu, *Mutat Res.* 2011, **721**, 184–191.
- 26 L. García-Hevia, R. Valiente, J. González, J. L. Fernández-Luna, J. C. Villegas, M.L. Fanarraga, *Curr. Pharm. Des.* 2015, **21**, 1920–1929.
- 27 E. González-Lavado, N. Iturrioz-Rodríguez, E. Padín-González, J. González, L. García-Hevia, J. Heuts, C. Pesquera, F. González, J. C. Villegas, R. Valiente and M. L. Fanarraga *Nanoscale* 2018, **10**, 11013–11020.
- 28 L. García-Hevia, J. C. Villegas, F. Fernández, I. Casafont, J. González, R. Valiente, M. L. Fanarraga, *Adv. Healthc. Mater.* 2016, **5**, 1080–1087.
- 29 M. L. Di Giorgio, S. Di Bucchianico, A. M. Ragnelli, P. Aimola, S. Santucci, A. Poma, *Mutat Res. Genet. Toxicol Environ Mutagen.* 2011, **722**, 20–31.
- 30 M. Ghosh, A. Chakraborty, M. Bandyopadhyay, A. Mukherjee, *J Hazard Mater.* 2011, **197**, 327–336.
- 31 J. Cveticanin, G. Joksic, A. Leskovac, S. Petrovic, A. V. Sobot, O. Neskovic, *Nanotechnology* 2010, **21**, 015102.
- 32 L. M. Sargent, A. F. Hubbs, S. H. Young, M. L. Kashon, C. Z. Dinu, J. L. Salisbury, S.A.Benkovic, D.T.Lowry, A.R.Murray, E.R.Kisin, K.J.Siegrist, L.Battelli, J.Mastovich, J.L.Sturgeon, K.L.Bunker, A.A.Shvedova, S.H.Reynolds, *Mutat Res – Genet Toxicol Environ Mutagen.* 2012, **745**, 28–37.
- 33 L. Gonzalez, I. Decordier, M. Kirsch-Volders, *Biochem Soc Trans.* 2010, **38**, 1691–1697.
- 34 A. A. Alizadehmojarad, X. Zhou, A. G. Beyene, K. Chacon, Y. Sung, M. P. Landry, L. Vuković, <https://doi.org/10.1101/2020.02.08.939918> [Pre-print - bioRxiv].
- 35 X. Li, Y. Peng, X. Qu, *Nucleic Acids Res.* 2006, **34**, 3670–3676.
- 36 H. Shams, B. D. Holt, S. H. Mahboobi, Z. Jahed, M. F. Islam, K. N. Dahl, M. R. K. Mofrad, *ACS Nano*. 2014, **8**, 188–197.
- 37 B. D. Holt, P. Short, A. D. Rape, Y. L. Wang, M. F. Islam, K. N. Dahl, *ACS Nano* 2010, **4**, 4872–4878.
- 38 Y. Dong, H. Sun, X. Li, X. Li, L. Zhao, *J Nanosci Nanotechnol.* 2016, **16**, 2408–2417.
- 39 Y. Liu, Y. Zhao, B. Sun, C. Chen, *Acc Chem Res* 2013, **46**, 702–713.
- 40 L. Migliore, D. Saracino, A. Bonelli, R. Colognato, M. R. D'Errico, A. Magrini, A. Bergamaschi, E. Bergamaschi *Environmental and Molecular Mutagenesis.* 2010, **51**, 294–303.
- 41 A. Kavosi, S. H. Ghale Noei, S. Madani, S. Khalighfard, S. Khodayari, H. Khodayari, M. Mirzaei, M. R. Kalhori, M. Yavarian, A. M. Alizadeh, M. Falahati, *Scientific Reports* 2018, **8**, 8375.
- 42 A. Fraczek, E. Menaszek, C. Paluszkiwicz, M. Blazewicz, *Acta Biomaterialia* 2008, **4**, 1593–1602.
- 43 E. González-Domínguez, N. Iturrioz-Rodríguez, E. Padín-González, J. Villegas, L. García-Hevia, M. Pérez-Lorenzo, W.J. Parak, M.A. Correa-Duarte, M.L. Fanarraga, *Int. J.Nanomed.* 2017, **12**, 6317 – 6328. View Article Online  
DOI: 10.1039/D0AY01357A
- 44 B. I. Kharisov, O. V. Kharissova, U. Ortiz Méndez, *MRS online Proc. Lib. Arch.* 2014, **1700**, 109–114.
- 45 Y. Gogotsi, *J. of Raman Spec.* 2007, **38**, 728–736.
- 46 A. Fairuz Bin Omar, M. Zubir Bin MatJafri, *Sensors* 2009, **9**, 8311 – 8335.
- 47 B. Glomstad, D. Altin, L. Sorensen, J. Liu, B. M. Jenssen, A. M. Booth, *Environ. Sci. Technol.* 2016, **50**, 2660.
- 48 B. Glomstad, F. Zindler, B. M. Jenssen, A. M. Booth, *Chemosphere* 2018, **201**, 269e277.

## A table of contents entry

View Article Online  
DOI: 10.1039/D0AY01357A

### Development of an accurate method for dispersion and quantification of carbon nanotubes in biological media.

Lorena González-Legarreta, Carlos Renero-Lecuna, Rafael Valiente and Mónica L. Fanarraga



A complete method to disperse, functionalize and quantify accurately carbon nanotubes for biological applications in nanomedicine is developed and described.

1  
2  
3  
4  
5  
6  
7  
8  
9  
10  
11  
12  
13  
14  
15  
16  
17  
18  
19  
20  
21  
22  
23  
24  
25  
26  
27  
28  
29  
30  
31  
32  
33  
34  
35  
36  
37  
38  
39  
40  
41  
42  
43  
44  
45  
46  
47  
48  
49  
50  
51  
52  
53  
54  
55  
56  
57  
58  
59  
60